experience. Fortunately, lacquer products are now available in spray cans which will simplify the application.

Various cleaning tests have been performed either at La Silla or Garching. Figure 2 shows the cleaning efficiency of the CO_2 snowflake and peeling technique on a mirror exposed to dust contamination. Recent scattering and reflectivity measurements have been performed on test mirror samples with four conditions of the mirror surfaces, the original coating being protected with a cover to obtain the reflectivity and scattering reference of data, half the dirty surface then cleaned with CO_2 jet and peel-off-lacquer. The results confirm the efficiency of the two procedures.

A project for an automated pilot CO_2 cleaning device for the NTT main mirror is at the stage of a call for tender at the ESO Headquarters. Mirror cleaning will be performed with CO_2 snowflake jets on a rotating arm.

Cooperation concerning the cleanliness of the observatory, telescopes and instruments will be greatly appreciated. Maximum efficiency in astronomical observations make these efforts mandatory.

Adaptive Filtering of Long Slit Spectra of Extended Objects

G. RICHTER[1,2], G. LONGO[2], H. LORENZ[1], S. ZAGGIA[2]

[1]*Astrophysical Institute, Potsdam, Germany*

[2]*Astronomical Observatory of Capodimonte, Naples, Italy*

1. Introduction

In both galactic and extragalactic astronomy, long-slit spectroscopy has proven to be a useful tool to study the physical properties of extended objects.

In the last two decades, CCD detectors coupled to spectrographs, while on the one hand simplifying some aspects of the processing of 2-D spectra – such as, for instance, the need for correcting the S-distorsion introduced by the image tubes –, on the other hand have allowed to reach fainter light levels thus arising the need for a careful removal of all sources of noise.

One of the most extreme examples is the study of the kinematical properties of the stellar component in early type

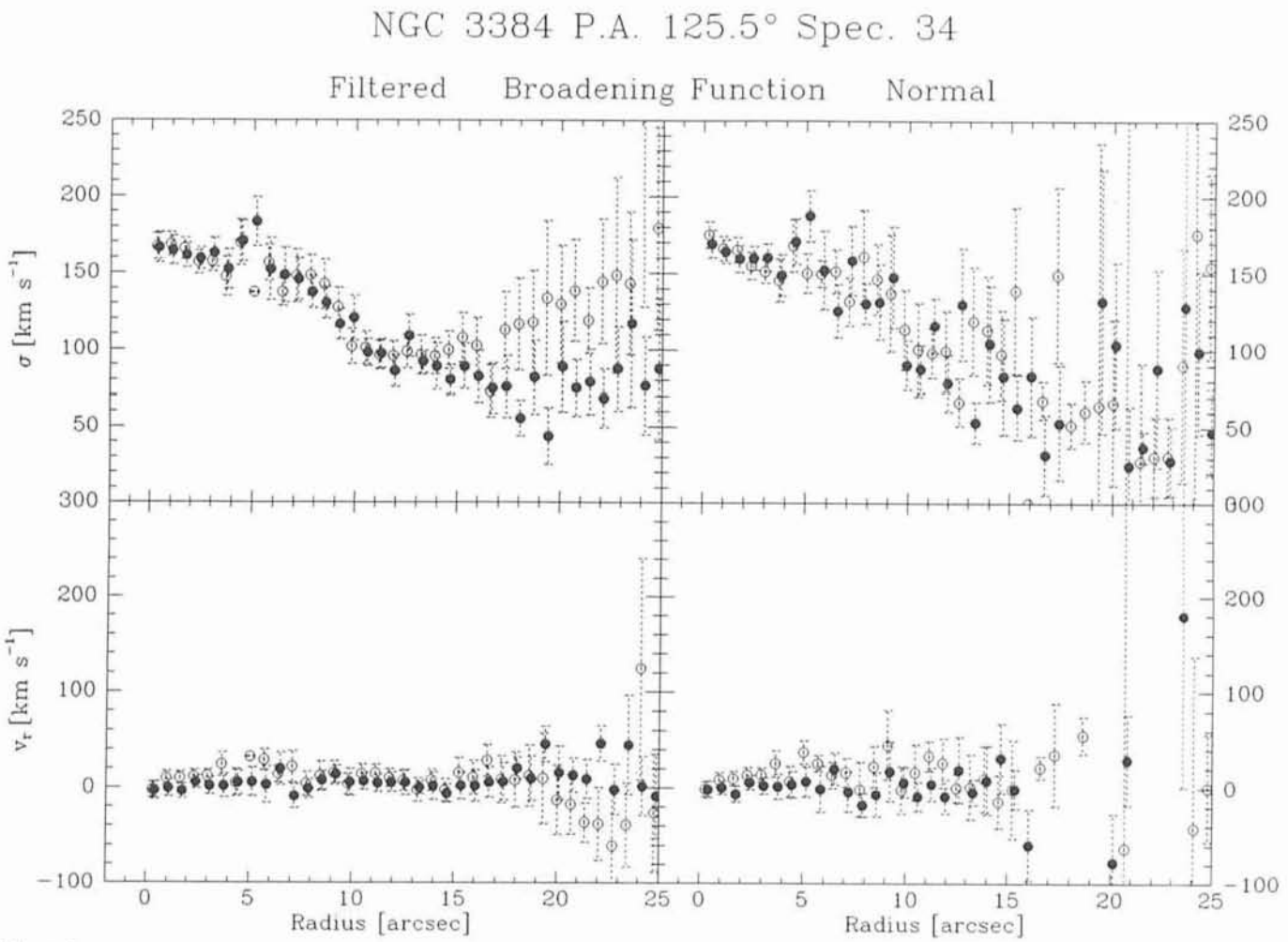

Figure 1.

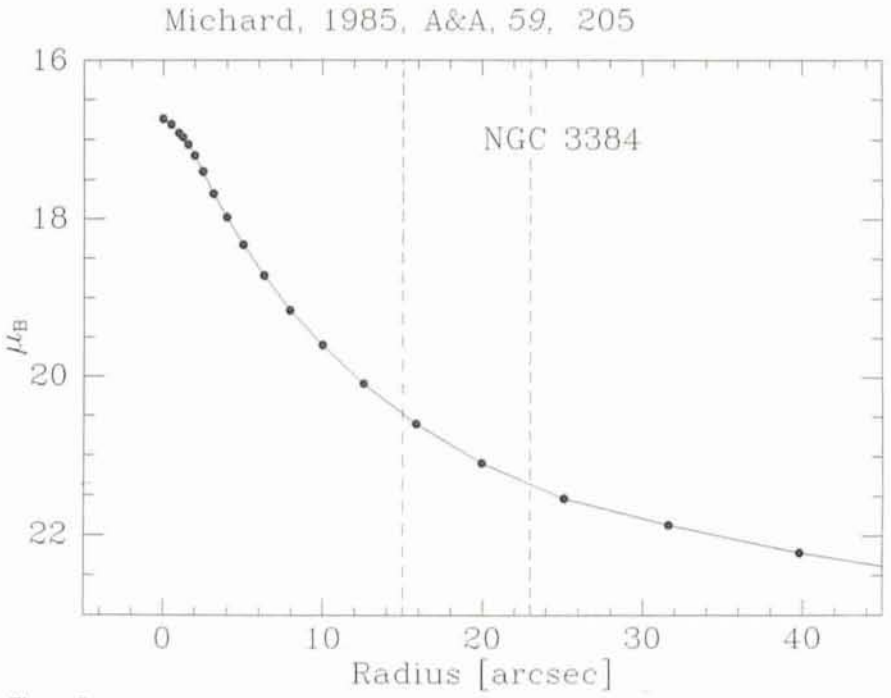

Figure 2.

galaxies or in the bulges of spirals by means of faint absorption features. As pointed out by several authors (Capaccioli and Longo, 1990; Kormendy and Djorgovski, 1989; Busarello et al., 1992), the understanding of the intrinsic structure, dynamics and overall properties of early-type galaxies requires to have radial velocity curves and velocity dispersion profiles as much extended as possible. Unfortunately, the fact that absorption lines are broadened by the velocity dispersion of the stellar component and the sharp decrease with radius in the surface brightness of galaxies render very difficult to go beyond 1.0 ~ 1.3 effective radii, i.e. beyond the region where the sky background becomes dominant. It needs to be pointed out, however, that even in the few cases where distances as large as 2.0 effective radii could be reached by adopting special and very time consuming observing and data-reduction strategies (Cappellaro et al. 1989), the data could not be fully exploited.

This being mostly due to the fact that in usual data reduction, after the standard flat fielding, the correction for particle events and bad pixels have been performed and after the sky background has been corrected for, there is still a broadband component of the noise due to the read-out of the CCD and to the electron noise, which prevents us from reaching fainter levels of surface brightness.

In the case of absorption-line measurements, the standard analysis methods such as, for instance, the cross-correlation or the Fourier quotient techniques, have already some capability to overcome the noise but in the direction of the dispersion only. In the direction perpendicular to the dispersion, the noise reduction is problematic and the usual stationary filtering technique cannot be used without destroying the resolution in the central part of the galaxy. The only way to overcome this limitation is to build a filter having a reasonable window size in the outer and fainter parts of the spectrum and capable of adapting to the local resolution by shrinking in the inner parts. Such an adaptive filter, which recognizes the local resolution by using the first and the second derivative of the image and is based on the *H – transform*, has been developed and implemented for astronomical images by Richter (1978) and recently applied to the photometry of NGC3379 by Capaccioli et al. (1988).

In direct images, however, the structure of both the noise and of the signal is isotropic, while in the case of spectra, it is necessary to filter only in the direction perpendicular to the dispersion, and leave completely untouched the noise and the signal in the direction of the dispersion (where the analysis methods deal properly with the noise). After such a filter has been applied, the cosmic-ray events and the stronger noise peaks are left untouched. In order to remove them we applied a 3×3 pixels Laplace filter, which has the property to enhance all spikes over a more or less constant background. The subsequent comparison of each spike with the point-spread function allows to discriminate between signal and noise events.

Table 1: *Characteristics of the spectra*

Spectrum Id.	Object Id.	P.A.	exp. time	date	tel	λ range
69	NGC1553	69	4500	01/02/90	2.2	4660-5500
27	NGC3384	125	2820	12/04/89	1.52	4400-5800
34	NGC3384	126	5400	12/05/89	1.52	4400-5800
78	NGC7176	78	4500	07/15/90	1.52	4600-5600

Table 2: *Characteristics of the observed galaxies.*

Object Id.	Type	P.A.	B_T	$A_e/2$
NGC 1553	S0 pec.	150	10.28	60"
NGC 3384	LBS	53	10.85	25"
NGC 7174	S pec.	88	14.23	
NGC 7176	E pec.	–	12.34	

2. Results

In order to test the above-described procedure, we applied it to a set of spectra obtained with the ESO 1.52-m and 2.2-m telescopes plus the Boller and Chivens spectrographs during several observing runs in 1989 and 1990.

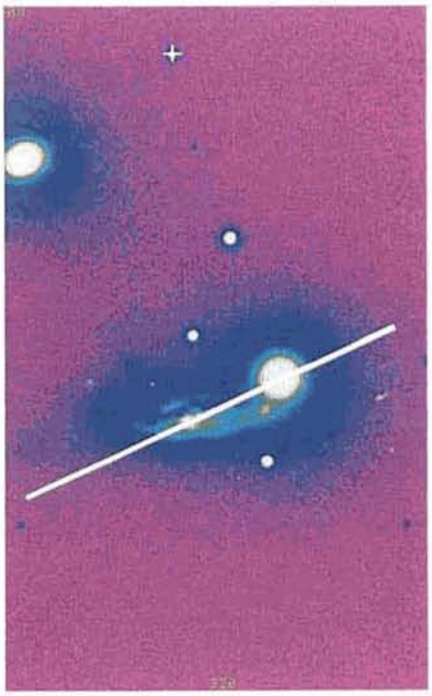

Figure 3.

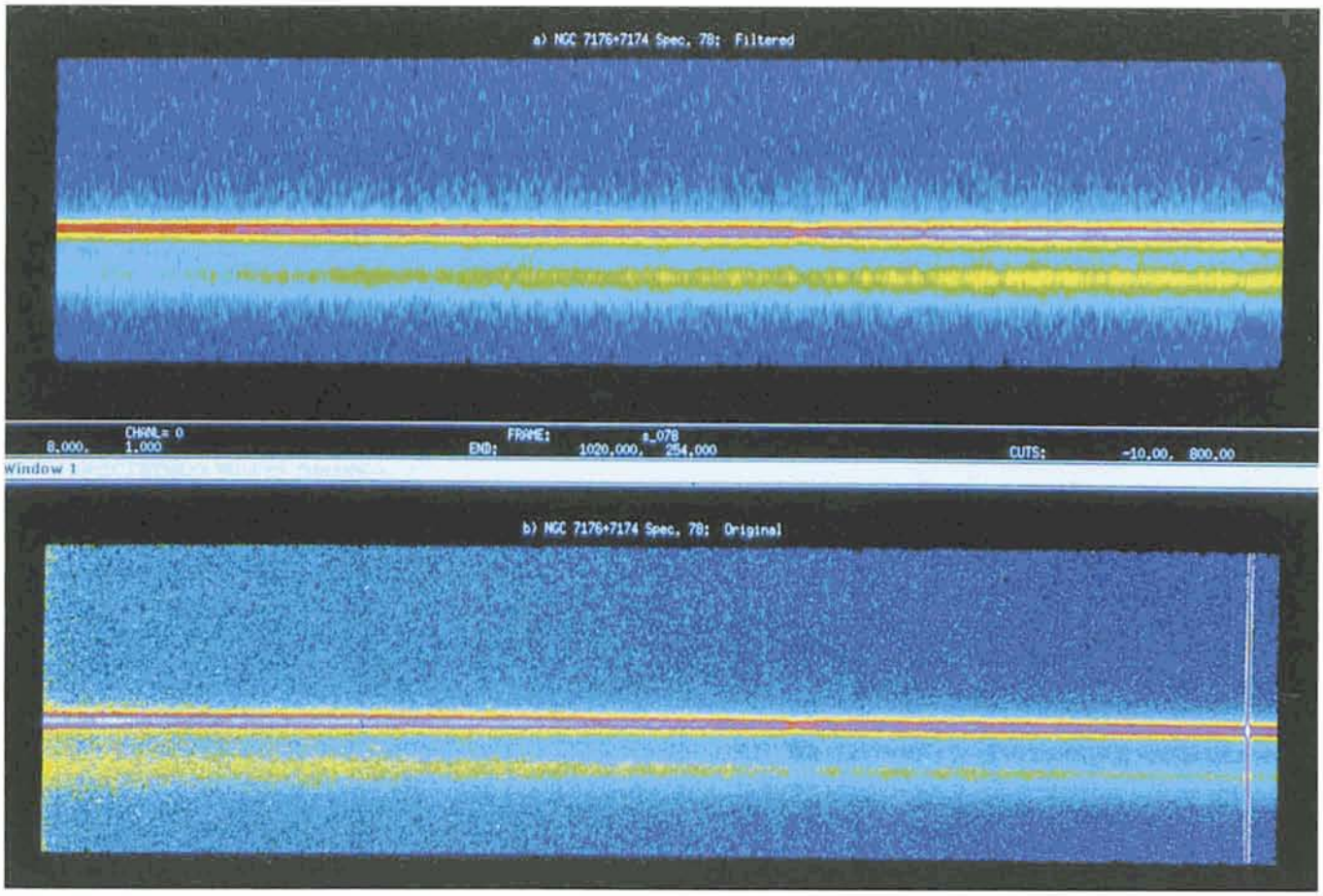

Figure 4.

The spectra were taken as a part of a project on the kinematics of early-type galaxies and are detailed in Table 1. Table 2, instead, gives some relevant information about the observed galaxies. Objects NGC7174 and NGC7176 belong to the Hickson group n. 90.

All spectra were processed twice: in a first reduction run, they were processed following standard MIDAS routines for flat fielding, bias and dark subtraction, sky background subtraction and wavelength calibration. The spectra were then analysed using the Fourier correlation quotient method kindly made available to us by Bender (1990), which consists in the deconvolution of the peak of the galaxy vs. template cross-correlation function with the peak of the autocorrelation function of the template star. In the second reduction run, after the standard pre-processing, the spectra were filtered accordingly to the procedure described in the previous paragraph and then analysed exactly in the same way as in the first case.

Figure 1 shows the radial velocity (bottom) and the velocity dispersion profiles (top) obtained from spectrum 34. Both profiles are folded over the photometric baricentre, and the opposite sides of the galaxy are marked with different symbols. "Filtered" data are

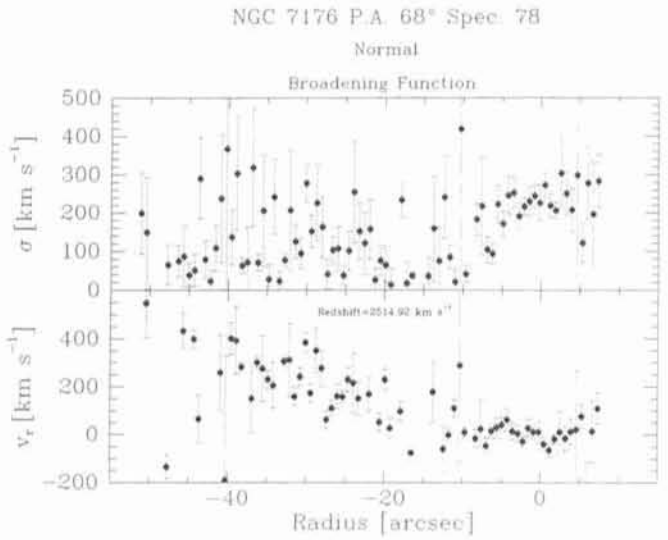

Figure 5.

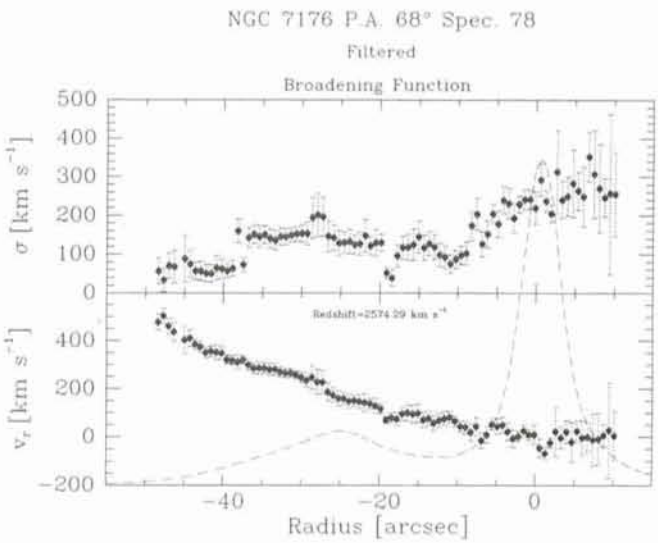

Figure 6.

shown on the left side, while normal – i.e. "unfiltered" – data are on the right one. The spectrum was taken at a position angle differing very little from the direction of the minor axis of NGC3384 and, as expected, no rotation is found. Even though the definition of the last meaningful point is somewhat arbitrary, it is evident that, even with a conservative estimate, the filtered data extend out to 23 arcsec, while the normal data reach out to about 15 – 16 arcsec. The comparison with the luminosity profile given in Figure 2 shows that the adaptive filtering of the data allows to go almost 1 magnitude fainter in surface brightness than with the normal approach. In the inner region, the two sets of data match very well even though the internal error in the filtered data is much smaller.

The fact that adaptive filtering is very effective at very low light levels is confirmed by the results obtained for spectrum 78. Figure 3 is a CCD image of three members of the Hickson group n.90: the two bright ellipticals are NGC7173 (left) and NGC7176 (right), while the spiral close to the centre of the image is NGC7174. The line marks the position of the spectrograph's slit, which covered both NGC7176 and NGC7174, Figure 4a shows the raw image of spectrum 78, while Figure 4b shows the same spectrum after preprocessing and adaptive filtering. Figures 5 and 6 give, respectively, the radial velocity and the velocity dispersion profiles in the "unfiltered" and "filtered" cases. The overimposed solid line gives the luminosity profile along the slit in an arbitrary scale.

An empirical test of the reliability of the results may be inferred by the comparison of Figure 7, which gives the radial velocity curve obtained from the "filtered" spectrum n.27, and the curve

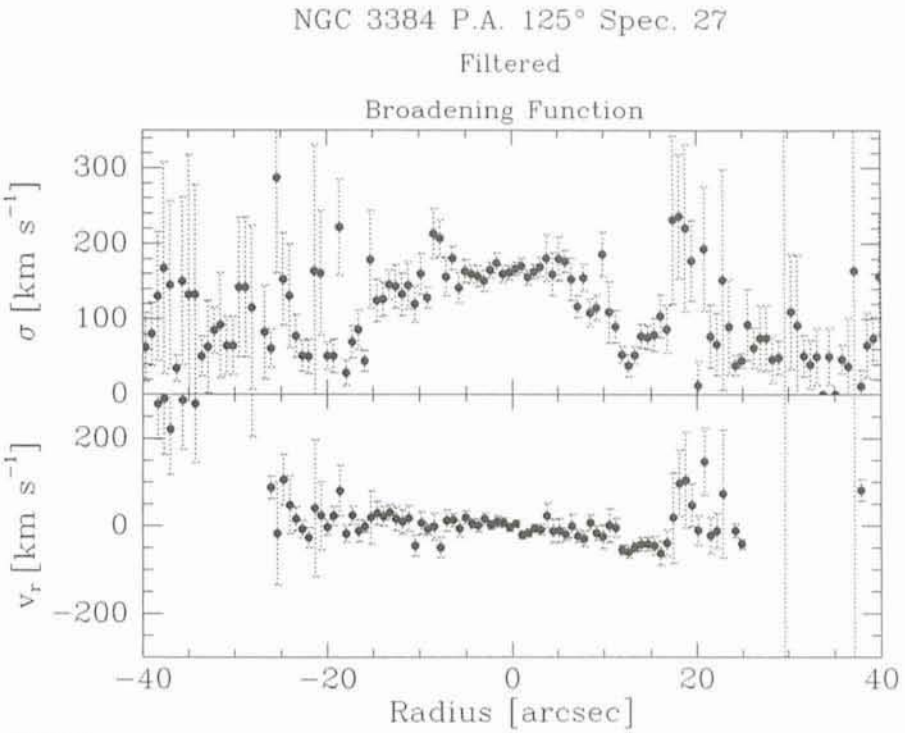

Figure 7.

(obtained from spectrum n.34) shown in Figure 1.

The different exposure times imply that the same signal-to-noise ratio is reached in spectrum 34 at a level 0.7 magnitudes fainter than in spectrum 27, thus partially compensating the effects of the filtering procedure. The match between the two radial velocity curves is quite good. A further test of the reliability of the method is shown in Figures 8 and 9, where the radial velocity curve of NGC1553 obtained by filtering spectrum 69 is compared to the rotation curve published by Kormendy (1984 = K84). The K84 data were obtained by using the 4-m KPNO telescope+RC spectrograph+image tube+Kodak IIIa-J, with a spectral resolution comparable to our set of data. The total exposure time for K84 was 6.5 hours. Taking into account that the quantum efficiencies of the two instrumental set-ups are more or less comparable and that both the collecting area and the exposure time are largely in favour of the K84 data, the good agreement between the two sets of data is a striking confirmation of the reliability of the adaptive filtering technique.

Acknowledgements

This work was partially sponsored by the Italian Space Agency (A.S.I.). G.R. acknowledges a grant by the Italian

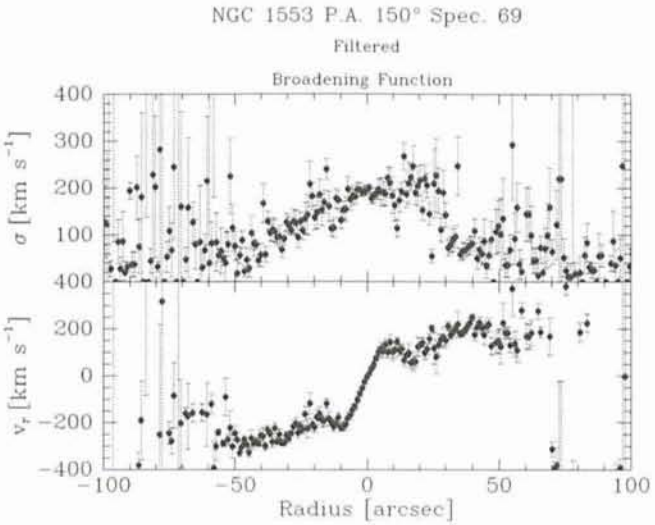

Figure 8.

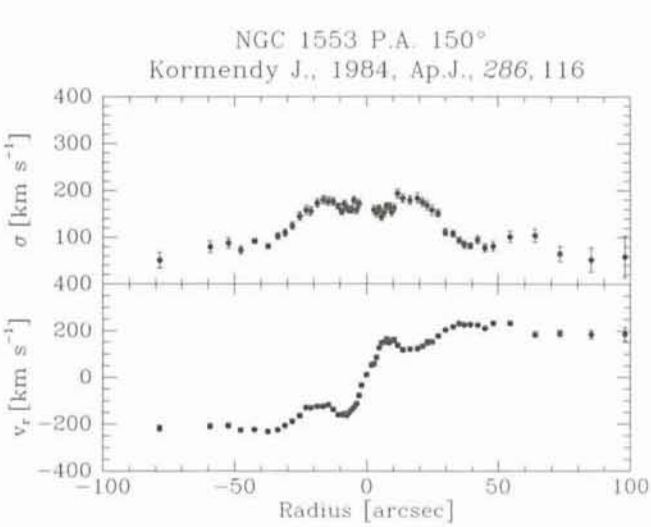

Figure 9.

CNR (National Council of Research); S.Z. acknowledges DIGITAL-Italia for granting a fellowship.

References

Busarello, G., Longo, G., Feoli, A. 1992, *Astron. Astrophys.*, in press.
Capaccioli, M., Caon, N. 1992, in *Morphological and Physical Classification of Galaxies* (Reidel, Dordrecht), p. 314.
Capaccioli, M., Longo, G. 1990, in *Windows on Galaxies*, Fabbiano G. et al. eds., p. 23, (Dordrecht, Holland).
Capaccioli, M., Held, E.V., Lorenz, H., Richter, G.M., Ziener, R. 1988, *Astron. Nachr.*, **309**, 69.
Cappellaro, E., Capaccioli, M., Held, V. 1989, *The Messenger*, **58**, 48.
Kormendy, J. 1984, *Astrophys. J.*, **286**, 116.
Kormendy, J., Djorgovsky, S.B. 1989, *Ann. Rev. Astron. Astrophys.*, **27**, 31.
Richter, G. 1978, *Astron. Nachr.*, **299**, 283.

The Determination of the Dead-Time Constant in Photoelectric Photometry

E. PORETTI, Osservatorio Astronomico di Brera, Milano, Italy

It is a well-known fact that raw counts measured at the output of a photon-counting photometer must be corrected for the dead-time constant τ. This correction originates from the finite time interval necessary for the electrons to cross the photomultiplier tube and, overall, from the time necessary to the amplifier/discriminator electronic to record the output pulse. From a practical point of view, this means that the instrumentation cannot resolve two incident photons separated by a time shorter than τ since they will be counted as a single event. Hence, the output counts will always be an underestimate of the input value.

Photons are travelling clumped together in space and the correction term can be calculated by means of the Bose-Einstein population statistics. The probability density f(t) that two photons arrive separated by a time t is

$$f(t) = \lambda e^{-\lambda t}$$

where λ is the arrival frequency of the photons. n_τ, the number of photons which arrive in a time interval shorter than τ, is given by

$$n_\tau = N \int_0^\tau f(t)dt = N \int_0^\tau \lambda e^{-\lambda t}\, dt,$$

while N is the total number of photons arrived during the measurement time. If it is 1 s, we have $N = \lambda$. By integrating, we obtain

$$n_\tau = N(1 - e^{-N\tau})$$

and, if we indicate as n the photons actually counted,

$$n = N - n_\tau = \frac{N}{e^{N\tau}}$$

This is the relation between the number of incident photons N and the number of counted photons n. If we can suppose that $N\tau$ is small, we can approximate $e^{N\tau}$ with a McLaurin development stopped at the first order, obtaining

$$n = \frac{N}{1 + N\tau} \qquad N = \frac{n}{1 - n\tau}$$

The latter is the formula most widely used in data-reduction routines. The value of the τ constant is generally supplied by the manufacturer and it is reported in the users manuals without any further checks. In general this assumption is justified by the impossibility to perform accurate laboratory tests. In some cases, the dead-time constant is confused with the rise time (i.e. the time interval during which the output rises from 10% to 90% of peak output) and its value is therefore underestimated. In the dome, astronomers can directly calculate τ by measuring two standard stars, one much brighter than the other, and comparing the observed Δm with the expected one.

However, this method requires a very precise knowledge of the magnitudes of the two stars and of the extinction coefficient. Cooper and Walker (1989, "Getting the measure of the stars", Adam Hilger Publ.) report a method which seems to me much more practicable. The telescope should be pointed towards sunrise and, when the sky is brightening, sky measurements should be performed alternating two different diaphragms, one much smaller than the other; let α be the ratio of their areas. An upper limit should be fixed to satisfy the following conditions: it should not be too high to cause damages to the photomultiplier or, from a more formal point of view, to invalidate the McLaurin development, but it should not be too small to make the linear fit described below uncertain. Weighting these factors, we can establish a maximum rate of $1.2\ 10^6$ counts per second. Sunrise should be preferred to sunset to better evaluate when this limit is reached and consequently not generate fatigue effects of the photomultiplier; as regards the observer's fatigue, moonlight can provide an alternative target . . . In any case, particular care must be taken to avoid expositions to very bright light sources. We have

$$N_l = \frac{n_l}{1 - n_l\tau} \qquad N_s = \frac{n_s}{1 - n_s\tau}$$

for the large and small diaphragm, respectively. In presence of a uniformly illuminated image (bright stars should be carefully excluded from the field of view), we can calculate

$$\frac{N_l}{N_s} = \alpha = \frac{n_l\ 1 - n_s\tau}{n_s\ 1 - n_l\tau}$$

and by means of simple passages

$$\frac{n_l}{n_s} = \alpha + \tau\ (1 - \alpha)n_l.$$

In a n_l vs n_l/n_s plane the last equation represents a line: the ratio of the diaphragm areas α is the intercept, while the angular coefficient allows us to calculate τ.

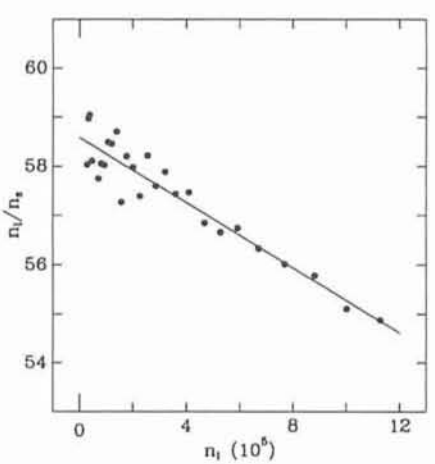

Figure 1.